Zoosyst. Evol. 100 (4) 2024, 1431–1442 | DOI 10.3897/zse.100.130288

PENSOFT

für Natur MUSEUM FÜR NATURKUNDE BERLIN

An update on the genus *Ischiomysis* with a description of *I. proincisa* sp. nov. (Crustacea, Mysida) from a sublittoral marine cave in the Gulf of Guinea (tropical E-Atlantic)

Karl J. Wittmann[1], Peter Wirtz[2]

1 *Department of Environmental Health, Medical University of Vienna, Kinderspitalgasse 15, A-1090 Vienna, Austria*
2 *CCMAR—Center of Marine Sciences, University of Algarve, Campus de Gambelas, 8005-139, Faro, Portugal*

https://zoobank.org/07A629AB-C1D1-45F3-995C-F114D8493685

Corresponding author: Karl J. Wittmann (karl.wittmann@meduniwien.ac.at)

Academic editor: Luiz F. Andrade ♦ **Received** 23 June 2024 ♦ **Accepted** 12 September 2024 ♦ **Published** 24 October 2024

Abstract

Ischiomysis proincisa **sp. nov.** is described from a comparatively large, semi-dark marine cave in sublittoral waters off the small island Ilhéu das Rolas, directly south of São Tomé Island in the Gulf of Guinea. As striking features, the new species is distinguished from both its congeners by an anteriorly incised rostrum in both sexes and by two versus only one modified flagellate spine on the ischium of the eighth thoracic endopod in males. The new species is sympatric yet ecologically remote from the congener *I. telmatactiphila*, which is associated with the sea anemone *Telmatactis cricoides* in brighter habitats. New records and morphological notes are given for *I. telmatactiphila* and *I. peterwirtzi*. An updated definition of the genus *Ischiomysis* and a key to its three species are given.

Key Words

Association with *Telmatactis cricoides*, equatorial E-Atlantic, first description, São Tomé Island, symbiotic species, troglophilic species

Introduction

Very large eyes, red body color (as in Fig. 2), freely swimming and forming small swarms as in the here first described mysid or even forming large swarms—such mysid life-form types can be encountered in small recesses, including empty mollusk shells, etc., up to very large caves. Detailed studies by Wittmann (1978) and Riera et al. (1991) on *Hemimysis speluncola* Ledoyer, 1963, *H. margalefi* Alcaraz, Riera & Gili, 1986, and *Sirielella gracilipes* H. Nouvel, 1942, in Mediterranean marine caves showed that these mysids seek shelter in dimly lit to dark zones during daytime and widely distribute over the sea floor for feeding and reproduction during the night. In the morning, they again seek shelter, often not returning to the same microhabitat. Part of the *S. gracilipes* population may remain in the phytal zone, hiding among algae. In analogy, many pelagic mysid species show diurnal vertical migration between euphotic, dysphotic, and aphotic zones (review in Mauchline 1980).

Mysids of the genus *Ischiomysis* Wittmann, 2013, were detected and described late in the taxonomic literature. This is probably because of the still early state of exploration of shallow coastal waters in the tropical E-Atlantic, whereas offshore waters were well-explored by great oceanographic expeditions such as the DIVA-1 expedition to the Angola Basin (Wittmann 2020). Both previously known species of *Ischiomysis* are associated with the club-tipped anemone *Telmatactis cricoides* (Duchassaing de Fonbressin, 1850), where they are easily spotted and sampled by divers. A photo (published by Wittmann 2013: Fig. 4) taken by Lisandro de Almeida

shows undetermined mysids with a similar habitus and red-orange body aggregated over the oral disc of a *T. cricoides* from the Island of Trindade in the tropical W-Atlantic, 1160 km off the coast of Brazil. Samples of this species are eagerly awaiting to determine its taxonomic affiliation, potentially with the genus *Ischiomysis*. That mysid and the present description of a new cave-dwelling species are an impetus to strengthen efforts in exploring the coastal fauna of the tropical Atlantic.

Materials and methods

Mysids were collected with diver-operated hand nets from the club-tipped anemone *Telmatactis cricoides* and in marine caves of São Tomé and São Vicente islands in the tropical E-Atlantic. Laboratory methods, definitions, and units of measurement as in Wittmann (2024). Expansion on slides makes the carapace appear wider but no longer compared with its shape *in loco*. Statolith diameters are measured as geometric means of apparent length and width in dorsal view. Artificial digital coloring of objects (by the camera system of the microscope) in Figs 4, 9 serves to visualize poorly contrasting details. Terminology as outlined by Wittmann (2024). Wilson (1989) defined "whip setae" (Fig. 7R) based on the basal part (handle) bearing a thin flagellum (cord) separated in the present context by an articulation, suture, or at least by an optically dense section upon standard microscopy. Wittmann et al. (2021) proposed to restrict the term "subrostral" to frontal processes between the rostrum and ocular symphysis and to use "epi-antennular" and "hypo-antennular" for frontal processes immediately above and below the antennular trunk (Fig. 5A), respectively. The hypo-antennular processes should not be confounded with a (here not treated) potential frontal process off the clypeus. The dorsal lobe (Fig. 5C) behind the distal margin of the terminal segment of the antennular trunk is termed the "disto-median lobe". Larval stages are distinguished according to Wittmann (1981).

Abbreviations and repository

BL body length measured from anterior margin of carapace to terminus of telson without spines
NHMW Natural History Museum of Vienna (repository)

Results

Systematics

Subfamily Heteromysinae Norman, 1892
Tribe Heteromysini Norman, 1892

Genus *Ischiomysis* Wittmann, 2013

Ischiomysis Wittmann, 2013: 489–492; San Vicente and Monniot 2014: 333, 340; Wittmann et al. 2014: 231, 309, 341; Wittmann and Wirtz 2017: 147; Daneliya 2021: 3, 6–7; Mees and Meland 2024: AphiaID 723169.

Short diagnosis. Shortened and updated from Wittmann (2013). Heteromysini with normal eyes, eyestalks without spiniform extension, no ocular papilla. Flagellate spine opposed by a large smooth seta on disto-mesial corner of terminal segment of antennular trunk; no modified spines (setae) on basal and middle segments. Appendix masculina short, with tuft of setae. Antennal scale well developed, with apical segment. Carapace (not counting rostrum) and mouthparts are normal. Thoracic sternites 2–8 without median processes in both sexes. Endopods 1–8 with distinct claw at apex. Third endopod specialized as gnathopod by forming a moderately strong subchela; carpus enlarged, not subdivided, armed with several flagellate spines. Fourth endopod with several weakly modified setae on carpopropodus and with apically bifid claw in both sexes. Endopod 8 only in males with a strong spiniform extension of praeischium and with 1–2 modified flagellate spine on ischium. Pleopods entire, reduced to small setose plates in both sexes; no spines or teeth. Uropods normal, with setae all around, no spine. Telson with spines on lateral margins; distinct apical cleft with spine-like laminae, no setae.

Species inventory. *I. peterwirtzi* Wittmann, 2013, from sublittoral rock recesses up to large marine caves, mostly observed associated with the club-tipped anemone *Telmatactis cricoides* but also distant from anemones at São Vicente Island and the small nearby island Ilhéu dos Pássaros in the Cape Verde archipelago, tropical E-Atlantic.

I. telmatactiphila Wittmann, 2013, close to *T. cricoides* in well-lit rock recesses at São Tomé Island and the small nearby islet Ilhéu de Santana, Gulf of Guinea, tropical E-Atlantic.

I. proincisa sp. nov. from a large semi-dark sublittoral cave at the coast of Rolas Island, close to São Tomé Island, in the Gulf of Guinea, tropical E-Atlantic.

Key to the species of the genus *Ischiomysis* (updated from Wittmann and Wirtz 2017)

1 Rostrum apically incised in both sexes; two flagellate spines on ischium of endopod 8 in males..... *I. proincisa* sp. nov.
– Rostrum entire in both sexes; only one flagellate spine on ischium of endopod 8 in males..... 2
2 Carapace anteriorly produced into a well-projecting triangular rostrum with rounded apex; exopod of uropods reaches with 18–25% of its length beyond telson; cleft of telson with spine-like laminae along basal 45–55% of its margins .... *I. telmatactiphila*
– Carapace with short rostrum forming a terminally rounded blunt angle; exopod of uropods reaches with 39–56% of its length beyond telson; cleft of telson with spine-like laminae along basal 80–86% of its margins .....*I. peterwirtzi*

Ischiomysis telmatactiphila Wittmann, 2013

Fig. 1

Ischiomysis telmatactiphila Wittmann, 2013: 492–497, 503–505, figs 1–3; San Vicente and Monniot 2014: tab. 1; Wittmann et al. 2014: 349, figs 18, 20; Bhaduri and Crowther 2016: tab. 1; Wittmann and Wirtz 2017: 132, 148; Saito et al. 2018: tab. 2; Wittmann and Ariani 2019: suppl.; Mees and Meland 2024: AphiaID 723174.

Material. São Tomé • 10 ♀♀ ad. (BL 4.2–5.4 mm), 6 ♂♂ ad. (BL 3.8–4.7 mm), 2 ♀♀ subad.; E-Atlantic, Gulf of Guinea, small islet Ilhéu de Santana; 0.2417°N, 6.7587°E; 15 m depth; 4 Feb. 2017; P. Wirtz leg.; well-lit fissure in exposed rock in front of the "Santana Tunnel", mysids above mouth disk of *Telmatactis cricoides* in crevice.

Note. The present record at the Ilhéu de Santana is the first after the first description. It extends the known distribution by 31 km air route across São Tomé Island or by >48 km waterway around São Tomé, respectively. Fig. 1 shows a dense swarm of this mysid species spread over the oral disc of *T. cricoides*. Additional mysid swarms were found closely associated with five other *Telmatactis* (above the oral disk and around the column of the anemone) in well-lit fissures of exposed rock in the Santana Bay at 0.2462°N, 6.7461°E. So far, no records of this species were made distant from anemones.

Figure 1. *Ischiomysis telmatactiphila* aggregated over the oral disk of *Telmatactis cricoides* in Santana Bay; photo P. Wirtz.

Ischiomysis peterwirtzi Wittmann, 2013

Figs 2, 3

Ischiomysis peterwirtzi Wittmann, 2013: 497–505, figs 5–6; San Vicente and Monniot 2014: tab. 1; Wittmann et al. 2014: 277, 349; Wittmann and Griffiths 2017: 40; Wittmann and Wirtz 2017: 132, 145, 148; Saito et al. 2018: tab. 2; Wittmann and Chevaldonné 2021: tab. 1, suppl.; Wittmann 2023: tab. S1; Mees and Meland 2024: AphiaID 723175.

Material. São Vicente • 6 ♀♀ ad. (BL 4.2–4.8 mm), 3 ♂♂ ad. (BL 4.1–4.4 mm), 2 ♀♀ subad.; E-Atlantic, Cape Verde archipelago, off Mindelo, small island Ilhéu dos Pássaros; 16.91147°N, 25.01181°W; 17 m depth; 26 Aug. 2015; P. Wirtz leg.; mysids around the basis of *Telmatactis cricoides* at foot of large stone • 3 ♂♂ ad. (BL 4.5–4.7 mm), 3 imm., 1 juv.; São Vicente, marine cave Furna da Rosa; 16.8500°N, 25.0833°W; 16 m depth; 5 April 2022; P. Wirtz leg.

Note. Cornea black in freshly caught specimens, eyestalks vary between transparent, opaque, and light red, cephalothorax and tail fan all over deeply red, pleon transparent to light red (ex-situ photo in Fig. 2), not considering colors of the content of foregut and intestine, in part visible through the (semi)-transparent body. The present records at the Ilhéu dos Pássaros and the cave Furna da Rosa are the first and second after the first description, respectively. They extend the known distribution by only 11 km to the NE. Swarms associated with *T. cricoides* (Fig. 3) as well

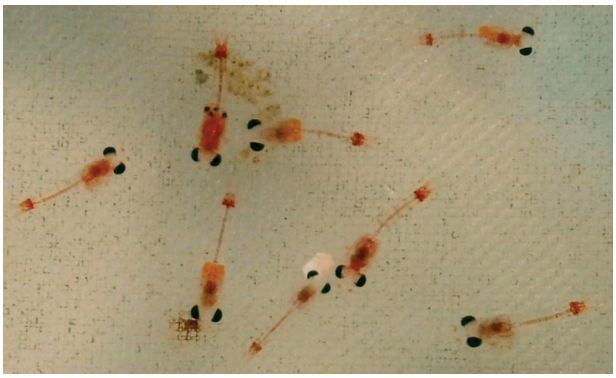

Figure 2. *Ex-situ* photo of living *Ischiomysis peterwirtzi* from small island Ilhéu dos Pássaros; photo P. Wirtz.

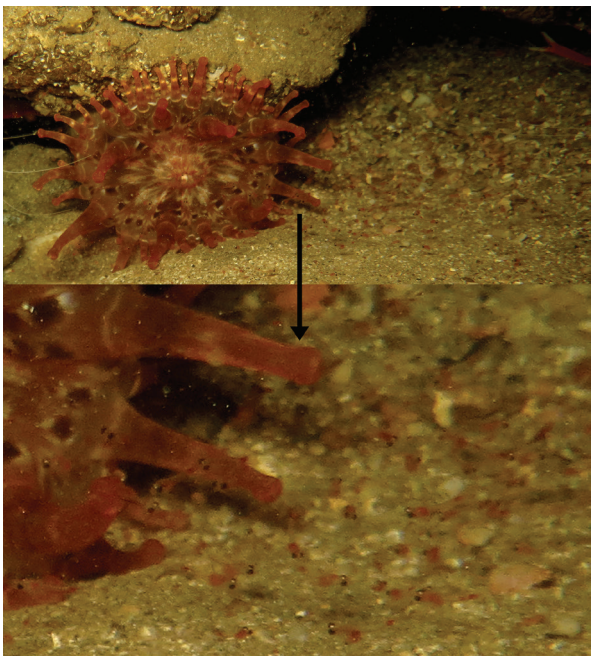

Figure 3. *Ischiomysis peterwirtzi* associated with *Telmatactis cricoides* in the marine cave Furna da Rosa; detail shows a swarm of this mysid species over sand and a small number of specimens over tentacles of the anemone; photo P. Wirtz.

as swarms distant from anemones were found in the large cave Furna da Rosa. Additional swarms were observed in five more submarine caves at São Vicente.

Ischiomysis proincisa sp. nov.

https://zoobank.org/88373DD6-43B0-4198-89ED-12344B6F3717

Figs 4–9

Type material. São Tomé • Holotype adult ♂ (BL 4.2 mm, NHMW-CR-30447), paratypes, 1 ♂ ad. (BL 3.7 mm), 1 ♂ subad., 1 ♀ subad., 2 imm., 1 juv. (NHMW-CR-30448); E-Atlantic, Gulf of Guinea, Ilhéu das Rolas (= small island crossed by the equator), off Ponta das Furnas (= cape); 0.0091°S, 6.5110°E; 19 m depth; 28 Aug. 2002, 9:50–10:10 local time; K.J. Wittmann leg.; V-shaped (i.e. two branches) semi-dark marine cave with three diveable entrances, from small mysid swarms in darker lateral recesses, diver operated hand net • Paratypes, 3 ♀♀ ad. (BL 4.0–4.3 mm), 13 ♂♂ ad. (BL 3.8–4.6 mm), 4 ♀♀ subad., 7 imm., 7 juv. (NHMW-CR-30448); 17 m depth; 22 Aug. 2002, 15:23–15:50 local time; remaining data as for holotype.

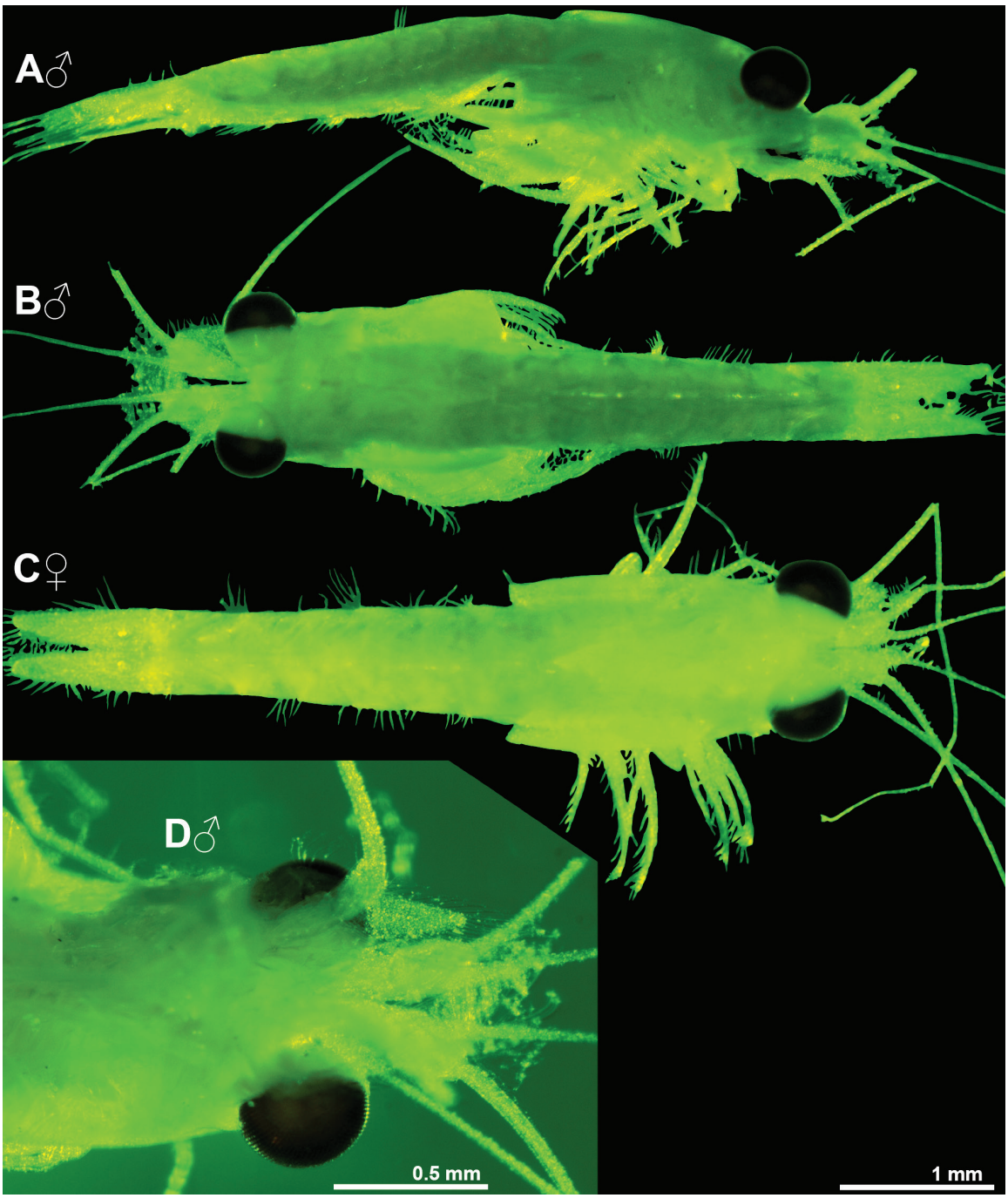

Figure 4. Habitus of *Ischiomysis proincisa* sp. nov.; holotype adult ♂ (BL 3.9 mm, **A, B, D**) and paratype adult ♀ (4.2 mm, **C**); **A, B.** Holotype *in toto*, lateral (A) and dorsal (B); **C.** Paratype *in toto*, dorsal; **D.** Cephalic region of holotype, ventral. **A–D.** Photos of fixed specimens, objects artificially separated from background, green coloring of objects artificial.

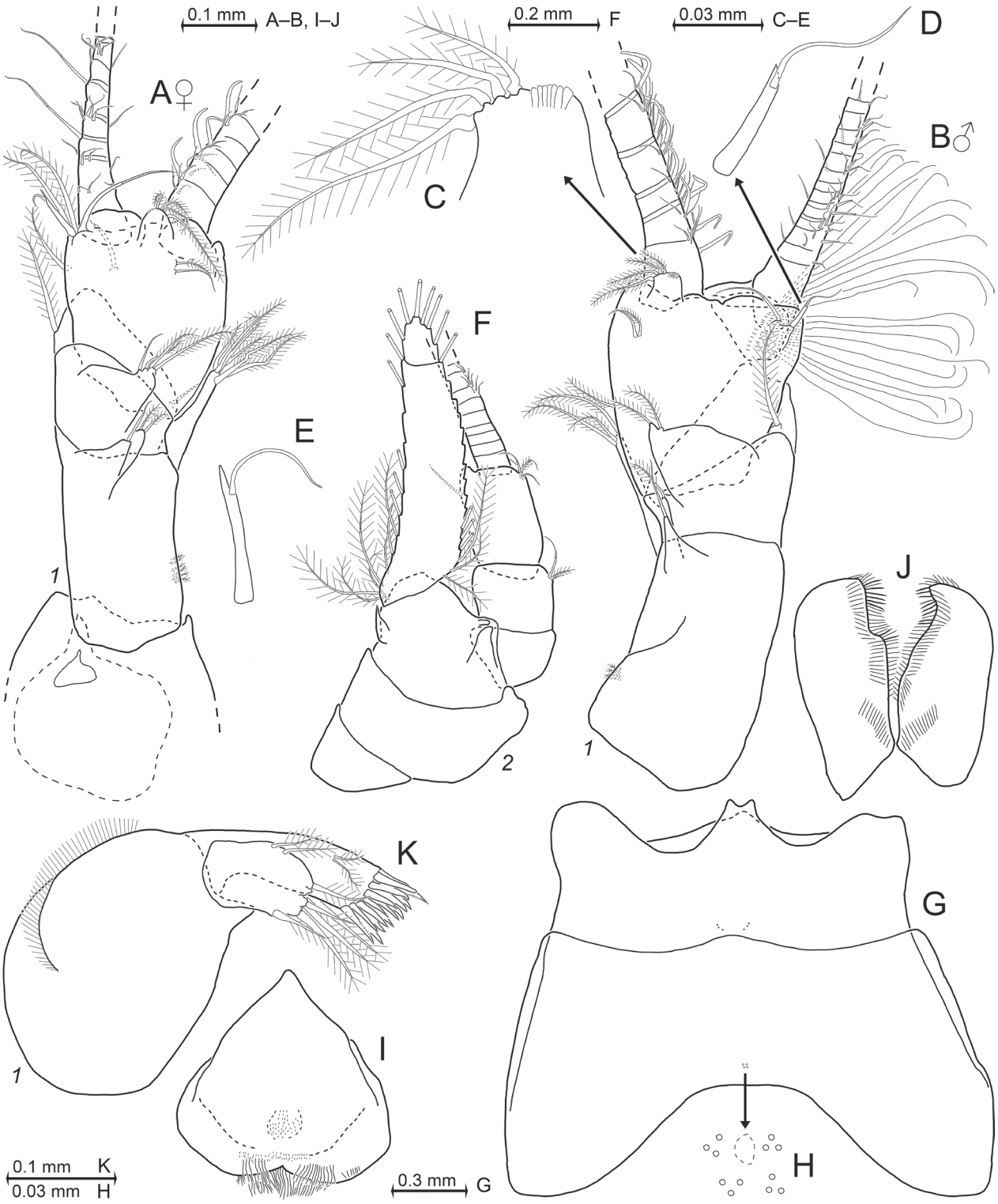

Figure 5. *Ischiomysis proincisa* sp. nov., paratypes adult ♀ (BL 4.3 mm, **A, E, I**) and adult ♂ (BL 4.5 mm, **B–D, F–H, J–K**); **A.** Right female antennula with associated processes from the frons, dorsal; **B.** Left male antennula, dorsal; details of the terminal segment of the trunk show the disto-median lobe (**C**) and the disto-mesial flagellate spine (**D**); **E.** Disto-mesial flagellate spine from left female antennula, dorsal; **F.** Antenna with antennal gland, dorsal, many setae omitted from the antennal scale; **G.** Carapace expanded on slide; **H.** Detail of (**G**) showing posterior pore group, pore diameters not to scale; **I.** Labrum, aboral face; **J.** Labium, frontal face; **K.** Maxillula, caudal.

Etymology. The species name is a Latin adjective with feminine ending, formed from the adjective *incisa* (incised) prefixed by the adverb *pro* (anteriorly), referring to the apically incised rostrum.

Type locality. Off cape Ponta das Furnas, 0.0091°S, 6.5110°E, in 17–19 m depth inside semi-dark marine cave. Each branch of the V-shaped cave is about 30 m long and open on both ends.

Diagnosis. Based on adults of both sexes. Large calotte-shaped cornea (Fig. 4) occupies distal 2/3 of eye surface (half eye length in dorsal view); cornea diameter is 28–35% carapace length. Rostrum trapezoid, anteriorly incised (Fig. 5G), about as long as the terminal segment of the antennular trunk. Only the terminal segment of the antennular trunk near disto-mesial edge with obliquely forwards oriented subapically flagellate spine with handle ending in a tooth-like projection (Fig. 5D); this spine opposed by a large smooth whip seta. Appendix masculina short though well developed, densely setose. Antennal scale (Fig. 5F) with small terminal segment separated by a not always distinct suture; scale reaching to the terminal margin of the antennular trunk; scale overreaching the antennal peduncle by 1/2 up to 2/3 of its length. Scale weakly bent laterally, slender; length is 4–5 times maximum width. Labrum (Fig. 5I) with distally narrowly rounded, roughly triangular rostral protrusion. Both sexes with small median lobe on thoracic sternite 1, no median processes on sterna 2–8 (Fig. 6E). Carpopropodus of thoracic endopods 1–8 with 2, 2, 2, 2, 3, 3, 3, and 3 segments (Fig. 6F, I, K, and Fig. 7L, P). Length of carpopropodus 3 is 4.0–4.5 times maximum width; carpus and propodus separated by a distinct suture (Fig. 7A, C). Carpus with 4 flagellate spines on distal fourth of its mesial margin in males (Fig. 7B) versus 5 spines on distal third in females (Fig. 7D). Propodus without spines. Carpopropodus of endopod 4 (Fig. 6K) with several simple smooth setae and 2–3 unilaterally barbed setae in two variants (Fig. 6L, M); claw almost straight, smooth, with bifid tip (Fig. 7G). Endopod 8 only in males with modified flagellate spine (Fig. 7M) on the outer margin of the ischium at one third ischium length from basis and an additional flagellate spine (Fig. 7N) basally on the inner margin; praeischium with a strong spiniform extension (Fig. 7O). Marsupium with large oostegite on thoracopods 7–8 plus a rudimentary plate on thoracopod 6. Penes tubular, terminally lobate (Fig. 6E); length without lobes is 3.5 times width; penes half as long as ischium of endopod 8. Pleopods (Fig. 8E–K) rudimentary, unsegmented, setose in both sexes, no spines. Uropods (Fig. 9A) setose all around, no spines. Exopod extends 14–27% its length beyond endopod and 28–44% beyond telson. Telson (Fig. 9B) length is 1.8–2.1 times maximum width and 1.0–1.2 times pleonite 6. Lateral margins with 13–18 spines only on distal half, not counting the apical spines. Telson with V-shaped narrow apical cleft penetrating 39–42% telson length; cleft with total of 30–37 spine-like laminae along basal 45–53% of its margins. Terminal lobes of telson each with two spines among which the disto-lateral spine is 14–15% telson length; the disto-mesial spine 0.3–0.4 times length of the disto-lateral spine. Telson with total of 31–37 spines.

Description. All features of the diagnosis. General appearance robust. Body red *in vivo*, length 3.7–4.6 mm in adult males (n = 15) and 4.0–4.3 mm in adult females (n = 3). Cephalothorax represents 28–33% body length, pleon without telson 51–56%, telson 11–12%, carapace without rostrum 20–26%, and rostrum 4–5%.

Eyes (Fig. 4). Eyestalks and cornea dorsoventrally compressed by a factor of 1.2. Cornea diameter twice the length of the apical segment of the antennular trunk. Eyestalks finely hispid by minute scales. Organ of Bellonci ellipsoidal, length 1/6 cornea diameter.

Carapace (Fig. 5G, H). The rostrum forms a distinct horizontal plate covering part of eyestalks. It reaches to 2/3 antero-posterior extension of normal-oriented eyestalks. Disto-lateral edges of the carapace well-rounded, anteriorly slightly produced. Posterior margin leaves the ultimate 1–1.5 thoracomere mid-dorsally exposed. As in many species of Mysidae, two characteristic groups of pores present on the midline of the carapace. The anterior group (Fig. 5G) is shortly in front of the cervical sulcus and comprises 6–10 pores with <1 μm diameter in symmetrical paramedian arrangement. The posterior pore group (Fig. 5G, H) is shortly in front of the posterior margin of the carapace; this group consists of 10–12 pores with about 2 μm diameter surrounding a larger but indistinct, rounded structure. Except for the here stated structures, carapace with smooth outer surface.

Antennulae (Fig. 5A–E). The trunk extends half its length beyond normal-oriented eyes. Measured along dorsal midline, the basal segment is 46–51% trunk length, median 18–20%, and terminal 30–34%. Basal segment of the antennular trunk (Fig. 5A, B) with two setose dorsal lobes (apophyses) near distal margin, in addition with a disto-lateral lobe; median and terminal segments each with one setose dorsal lobe near distal margin. Basal segment on basal half of its lateral face with 3–5 minute setae. The large barbed seta arising from the inner distal corner of the median segment not extending beyond the terminal segment in both sexes. The flagellum of the spine at the terminal segment of the antennular trunk inserts more apically in the male (Fig. 5D) compared to the female (Fig. 5E); this dimorphism also found in the congener *I. telmatactiphila*. Epi-antennular process (solid line in Fig. 5A) subtriangular with small, rostral, acute projection; hypo-antennular process (dashed line in Fig. 5A) subcircular with blunt subtriangular rostral projection.

Antennae (Fig. 5F). Sympod dorsally with terminally rounded, tongue-like process. Disto-lateral edge of sympod with tooth-like process. Sympod caudally with bulbous lobe containing end sac of antennal gland. Antennal scale setose all around. Apical segment, if distinct, contributes 11–16% to total scale length. Peduncle 0.7–0.8 times scale length but extending to only about half scale length due to its more caudal insertion. Basal segment is 24–29% the length of the peduncle, second is 27–31%, and third is 44–46%.

Primary mouthparts (Fig. 5I, J and Fig. 6A–C). Labrum (Fig. 5I) weakly cuticularized, densely covered by short, stiff bristles. Paragnaths (Fig. 5J) with moderately stiff bristles, no tooth-like bristles. Mandibular palp three-segmented (Fig. 6A). Its proximal segment without setae, 8–12% length of palp. Median segment: 63–65% palp length. Its length 3.0–3.7 times maximum width. Its lateral margin almost all along with 8–9 smooth setae, an additional basally barbed seta in distal-most position.

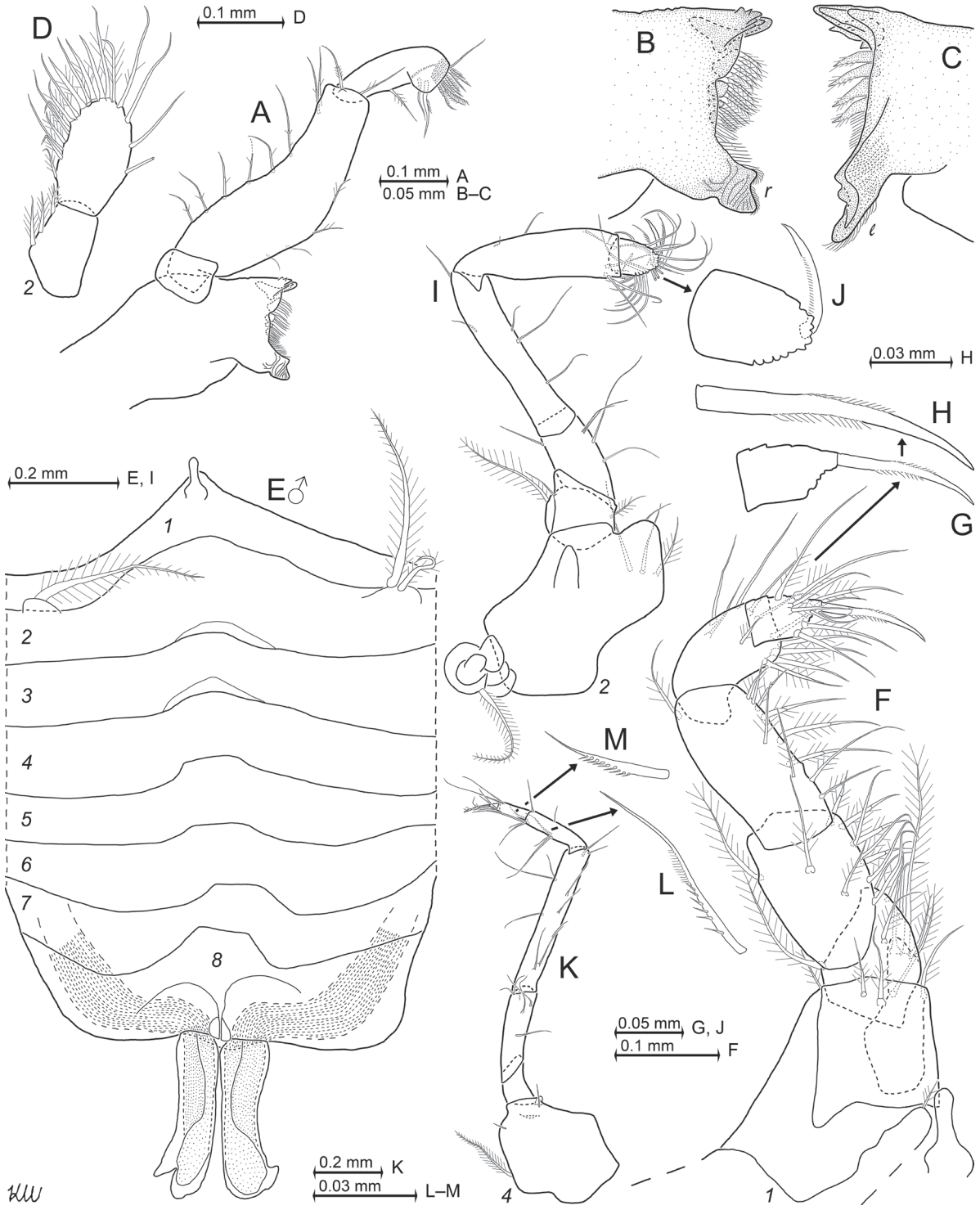

Figure 6. *Ischiomysis proincisa* sp. nov.; paratypes adult ♀ (BL 4.3 mm, **A–D**) and adult ♂ (BL 4.5 mm, **E–M**); **A.** Right mandible with palpus, caudal; **B, C.** Masticatory parts of right (**B**) and left (**C**) mandibles, caudal; **D.** Maxillary palp, rostral; **E.** Thoracic sternites 1–8 with penes, ventral; **F.** Thoracic endopod 1 with part of coxa, caudal; **G.** Detail of (F) showing dactylus 1 with claw, setae omitted; **H.** Secondary detail of (F) showing claw 1; **I.** Thoracic endopod 2, rostral; **J.** Detail of (I) showing dactylus 2 with claw, setae omitted; **K.** Thoracic endopod 4 with basis (sympod), rostral; **L, M.** Details of (K) showing modified setae of the carpus (**L**) and the propodus (**M**).

Mesial margin with 4–6 smooth setae distributed with mostly large interspaces. Terminal segment 27–28% palp length. Its mesial margin bare except for some setae near apex; distal half of lateral margin densely setose. Pars molaris with well-developed though comparatively small grinding surface in both mandibles. Left mandible (Fig. 6C) with pars incisiva bearing three teeth, digitus mobilis with two teeth, pars centralis with four basally thick, spiny teeth. Right mandible (Fig. 6B) with pars incisiva bearing 4–5 teeth, digitus mobilis with two teeth; pars

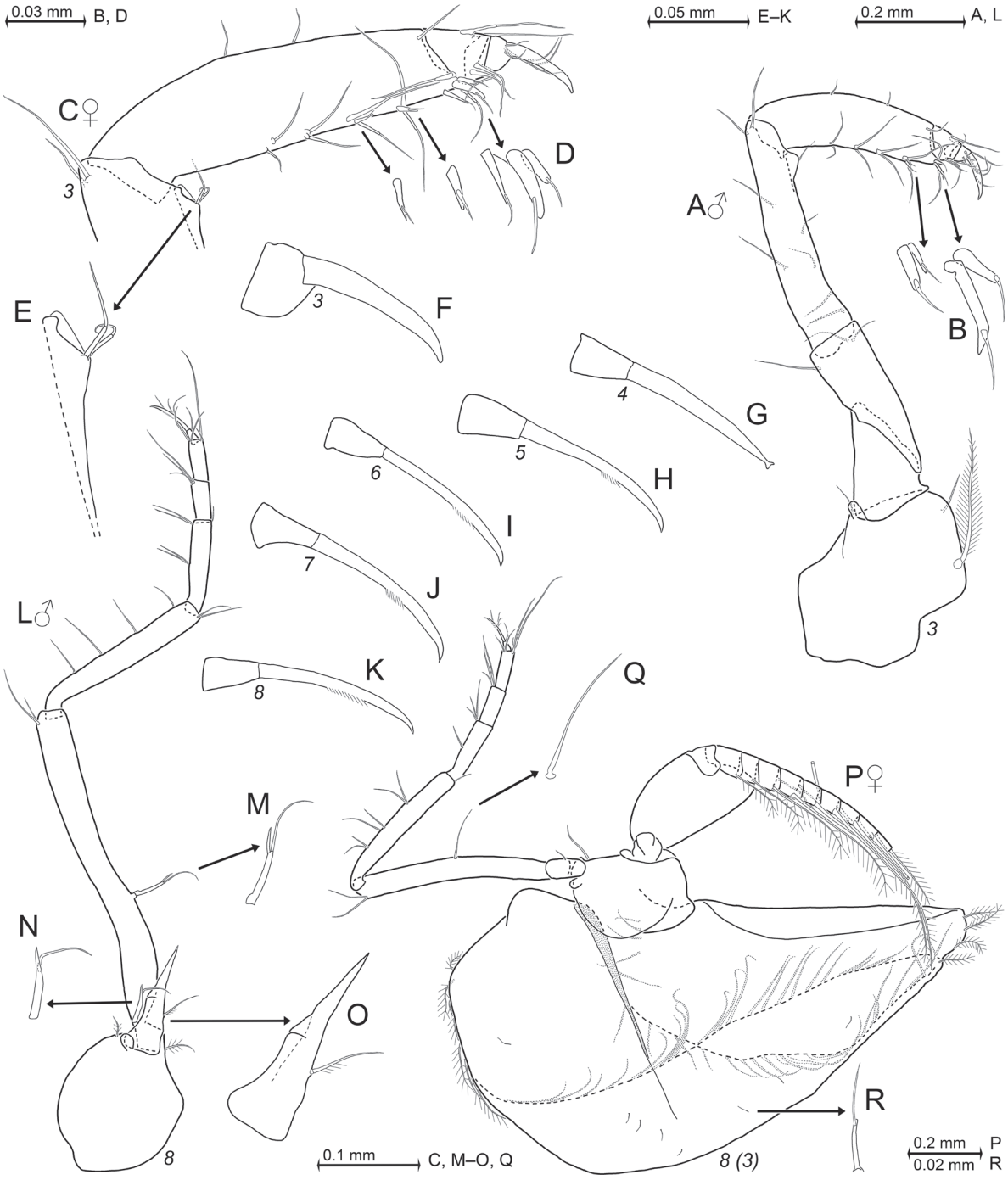

Figure 7. Thoracopods 3–8 in *Ischiomysis proincisa* sp. nov.; paratypes adult ♂ (BL 4.5 mm, **A, B, G–O**) and adult ♀ (BL 4.3 mm, **C–F, P–R**); **A.** Male thoracic endopod 3, rostral; details (**B**) show the flagellate spines of the carpus; **C.** Tarsus and distal portion of the merus in female thoracic endopod 3, rostral; details show the flagellate spines of the carpus (**D**) and the disto-mesial carina of the merus (**E**); **F–K.** Series of dactyli 3–8 with claw, setae omitted; **L.** Male thoracic endopod 8, caudal; details show the flagellate spines (**M, N**) of the ischium and the modified praeischium (**O**) with large tooth-like projection; **P.** Female thoracopod 8 with outer face of oostegite 3, lateral; details show a normal smooth seta (**Q**) of the ischium and a subapically flagellate whip seta (**R**) from the outer face of the oostegite.

centralis with 3–4 separate bases each bearing numerous slender spines that are bilaterally armed with stiff bristles. Bases decreasing in size and numbers of spines orally.

Foregut (Fig. 8A–D). Lateralia anteriorly with group of slender, apically coronate spines (Fig. 8A) with small denticles along distal <2/3 of the shaft. Lateralia more caudally with shorter, apically pronged spines (Fig. 8B) bearing small denticles along >2/3. Lateralia on each side of the foregut more caudally with cluster of 6–7 weakly, in part indistinctly serrated spines (Fig. 8C) of varying size. Dorsolateral infoldings each with cluster of three strong rugose spines (Fig. 8D).

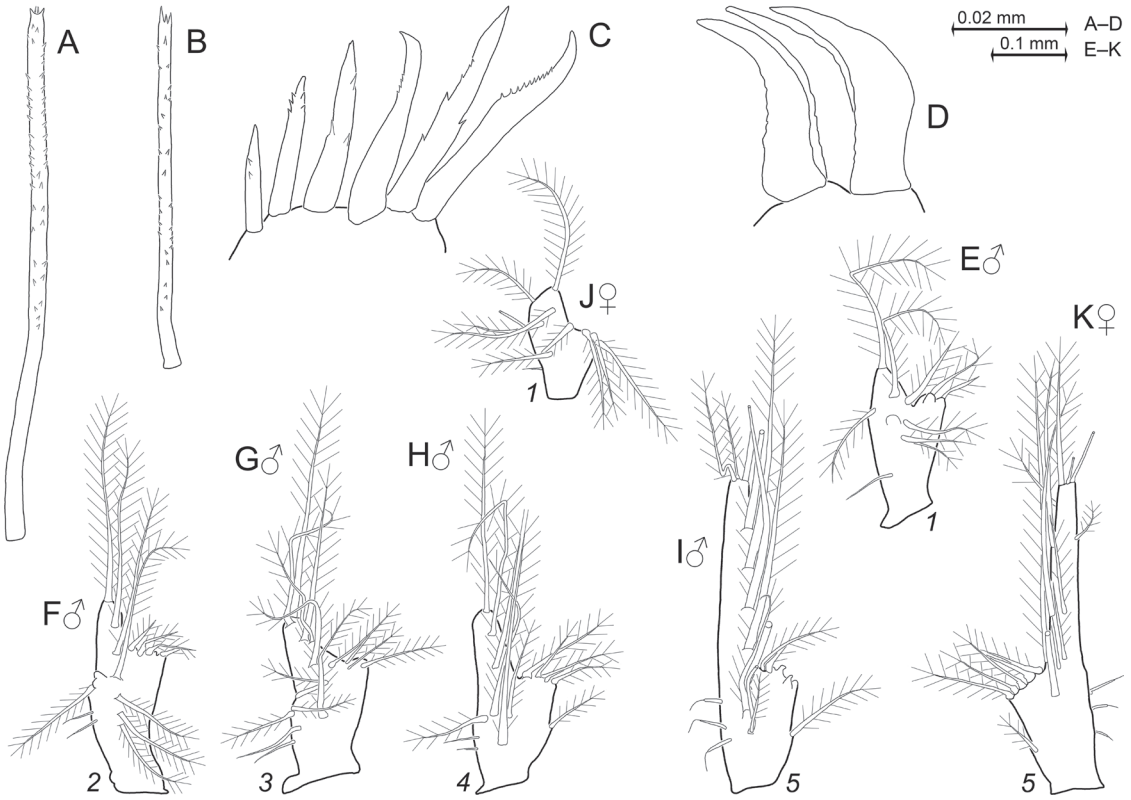

Figure 8. Spines of the foregut and pleopods in *Ischiomysis proincisa* sp. nov.; paratypes adult ♂ (BL 4.5 mm, **A–I**) and adult ♀ (BL 4.3 mm, **J, K**); **A–D.** Modified spines of the foregut in dorsal view, from the anterior (**A, B**) and posterior (**C**) parts of the lateralia and from dorsolateral infolding (**D**); **E–I.** Series of right male pleopods 1–5, lateral = rostral face; **J.** Right female pleopod 1, lateral; **K.** Left female pleopod 5, lateral.

Maxillula (Fig. 5K). Distal segment terminally with series of 10–11 strong spines, among which the two most peripheral spines are largest and subapically serrated, whereas the spines in between are weakly or not serrated. This segment subterminally with two short setae bearing long barbs on their distal 2/3; no pores detected near these setae. These setae not reaching the basis of the spines. Only two short setae also found in the congener *I. telmatactiphila*, whereas most Mysidae species show more and longer setae of that kind. Endite of the maxillula terminally with three large spiny setae accompanied by three shorter setae of that kind, caudal face with two small barbed setae.

Maxilla (Fig. 6D) with terminal segment of palp 1.6–1.8 times longer than wide and 1.3–1.6 times length of the basal segment. Terminal segment with densely setose mesial margin; only 3–4 setae along distal 2/3 of the lateral margin, no spines. Basal segment with three basally thick, barbed setae.

Thoracic sternites (Fig. 6E). Sternite 1 with small, about linguiform anterior lobe. Sternites 2–8 without median processes in both sexes. Sternite 2 with 1–3 barbed setae on intersegmental joint with thoracopod 2. Penes distally ending in 4 lobes, no setae.

Thoracopods in general (Fig. 6F–M and Fig. 7). Basal plate (Fig. 7P) of exopods expanded, length 1.5–1.9 times maximum width. Lateral margin of the plates ends in a broadly rounded corner. Flagellum of exopods 1–8 with 8, 9, 9, 9, 9, 9, 9, and 9 segments (Fig. 7P), respectively. Thoracopod 1 with large, leaf-like, smooth epipod. Basis (fused with sympod) of endopod 2 (Fig. 6I) with comparatively large lappet-like apophysis on rostral face; this apophysis small in endopods 3–8 (Fig. 6K and Fig. 7A, L, P); no such apophysis in endopod 1. Ischium shorter than merus in endopods 1–4 (Fig. 6F, I, K, and Fig. 7A), but longer than merus in endopods 5–8 (Fig. 7L, P). Thoracic endopods 1–2 each with dactylus (Fig. 6G, J) larger than that of endopods 3–8 (Fig. 7F–K); dactylus 3 (Fig. 7F) wider but not longer than dactyli 4–8 (Fig. 7G–K). Dactylus 1 with slender, weakly bent claw which is bilaterally "serrated" by stiff bristles along median portions (Fig. 6G, H). Claw 2 unilaterally rugose along proximal 2/3 (Fig. 6J). Claw 3 strong, somewhat bent, smooth (Fig. 7F). For claw 4, see "Diagnosis". Claws 5–8 weakly bent, "serrated" in subapical portions (Fig. 7H–K). Combined praeischium plus ischium of endopod 2 (Fig. 6I) are 0.6 times merus length, carpopropodus plus dactylus 1.1 times merus. Dactylus 2 very large, with dense brush formed by large numbers of normal setae and 6–10 modified setae, the latter apically bent, bearing double series of stiff barbs along proximal 2/3 to 3/4.

Gnathopods (Fig. 7A–F). Thoracic endopod 3 forms a powerful subchela. Basis with much shorter endite (Fig. 7A), if any, compared to that (Fig. 6I) of endopod 2. Ischium of endopod 3 is 2.6–3.0 times as long as wide; merus 4.5–5.1 times as long as wide and 1.4–1.6 times length of ischium. Ischium and merus strong, with smooth

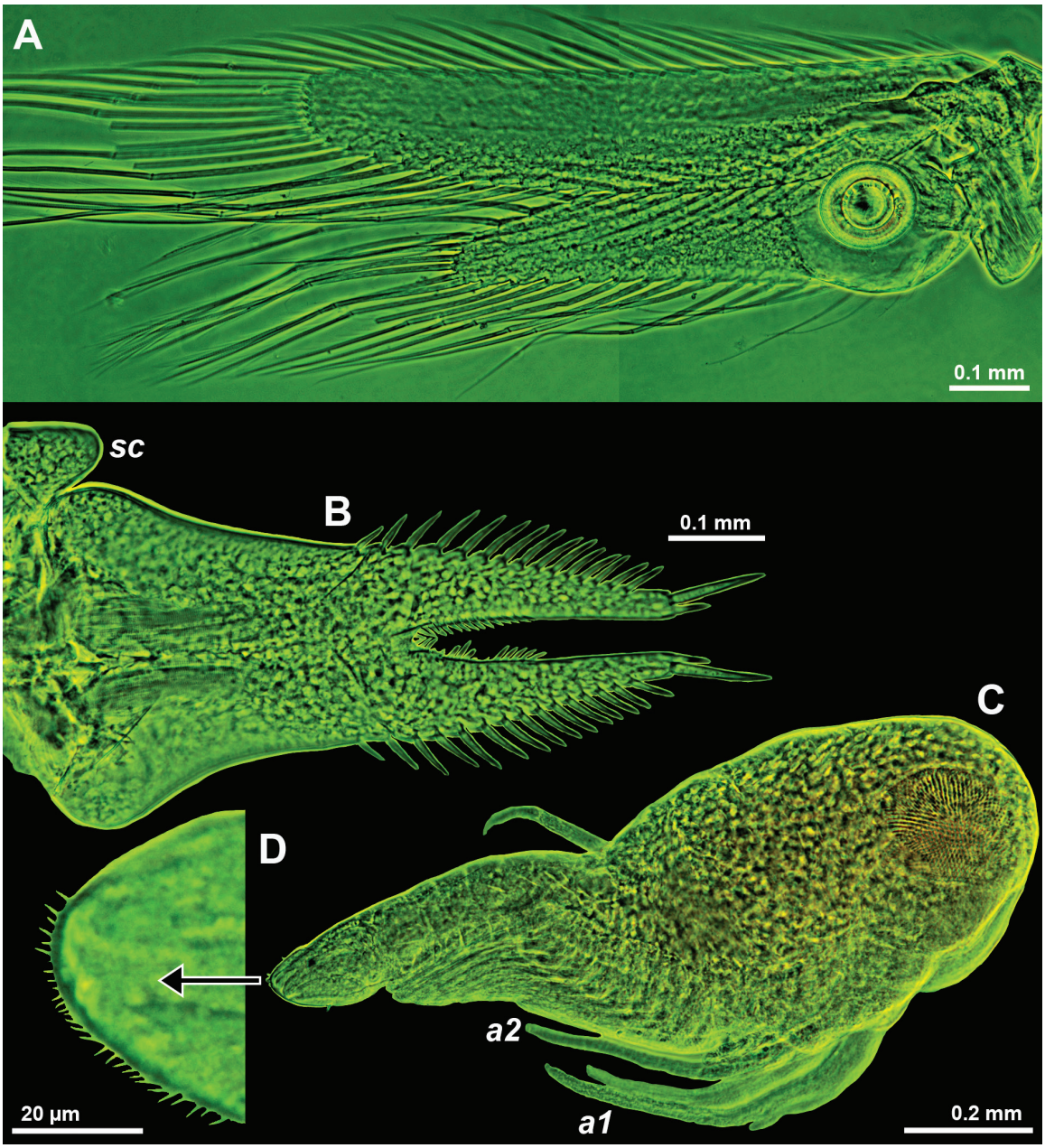

Figure 9. *Ischiomysis proincisa* sp. nov.; paratype adult ♂ (BL 4.5 mm, **A, B**) and nauplioid larvae (**C, D**); **A.** Uropods, ventral; **B.** Telson and right scutellum paracaudale (*sc*), ventral; **C.** Nauplioid larva at substage N4, lateral; lower case labels indicate antennula (*a1*) and antenna (*a2*); **D.** Tip of pleon in another nauplioid specimen. Panel (**A**) combined from two photos; **A–D.** Green coloring of objects artificial; **B–D.** Objects artificially separated from background.

setae only. Disto-mesial edge of merus with short longitudinal ridge bearing two setae (Fig. 7E). Carpopropodus as long as 0.8–0.9 times merus and 1.2–1.3 times ischium. Length of carpus 3.4–3.5 times maximum width.

Marsupium (Fig. 7P, R). Ultimate (third) oostegite rolled inwards to form two widely communicating sub-chambers. Its rostral and ventral margins with dense series of barbed (plumose) setae; inside with 5–9 microserrated setae close to the insertion on thoracic sympod 8; ventral half of oostegite 3 with about 7–10 small whip setae (Fig. 7R) loosely scattered over the outer surface.

Pleon (Fig. 8E–K). Pleomeres 1–5 measure 0.7–0.9, 0.6–0.8, 0.7–0.9, 0.6–0.9, and 0.7–0.8 times the length of pleomere 6, respectively; in other words, pleomere 6 is always shorter than combined pleomeres 4–5. Length without setae increases in series of pleopod 1, followed by subequal pleopods 2–4, and then by the much longer and slender pleopod 5. Pleopods 1–5 (Fig. 8E–K) mainly with plumose or barbed setae, but there are 1–3 smooth seta only in subbasal position on the outer margin; the latter setae clearly representing whip setae in pleopod 5 of both sexes. Pleopods 1–5 show no other types of setae, no extraordinarily long setae, no spines or teeth.

Tail fan (Fig. 9A, B). Scutellum paracaudale (labeled "*sc*" in Fig. 9B) forms a well-rounded shield covering the basolateral edge of the telson. Exopod of uropods (Fig. 9A): 4.9–5.6 times longer than broad, inner margin convex, outer margin very slightly concave, almost

Table 1. Morphological comparison between the species of *Ischiomysis*.

Characters	*I. peterwirtzi* Wittmann, 2013	*I. telmatactiphila* Wittmann, 2013	*I. proincisa* sp. nov.
BL (mm) of females	4.2–5.6	4.2–5.4	4.0–4.3
BL (mm) of males	3.5–5.1	3.5–4.7	3.7–4.6
Rostrum	short, widely rounded	triangular, apex narrowly rounded	trapezoid, anteriorly incised
Handle of flagellate spines on antennular trunk and on carpus of thoracic endopod 3	without distal projection	with tooth-like projection	with tooth-like projection
No. flagellate spines on carpus of thoracic endopod 3 in females	3	5	5
No. flagellate spines on carpus of thoracic endopod 3 in males	2	4	4
No. flagellate spines on ischium of thoracic endopod 8 in males	1	1	2
Ratio of penis length to width (without lobes)	2	3	3–4
Exopod of uropods reaches X% of its length beyond telson	39–56%	18–25%	28–44%
Ratio of telson length to maximum width	1.6–1.7	1.9–2.2	1.8–2.1
Ratio of bare portion to total length of lateral margins of telson	0.5–0.6	0.5	0.5
No. spines on each lateral margin of telson	5–7	11–14	13–18
Apical cleft penetrates X% telson length	27–34%	34–37%	39–42%
Telson cleft with laminae along basal X% of its margins	80–86%	45–55%	45–53%
Distribution	São Vicente and nearby island, Cape Verde archipelago, E-Atlantic	São Tomé and nearby island, Gulf of Guinea, E-Atlantic	Small island close to São Tomé, Gulf of Guinea, E-Atlantic
Microdistribution	Swarms associated with *Telmatactis cricoides*, also found distant from anemones inside marine cave	Swarms closely associated with *Telmatactis cricoides*	Small swarms in dimly-lit marine cave, no anemones detected
Depth (m)	8–17	15–46	17–19

straight, 1.2–1.4 times the length of endopod. Statoliths composed of fluorite; shape discoid, diameter 60–136 µm, maximum thickness 27–60 µm, statolith formula 2 + 3 + (5–7) + (1–2) + (4–5) = 15–19 (n = 12). Telson (Fig. 9B) shaped as in *I. telmatactiphila*, length is 1.1 times endopod of uropod and 0.8–0.9 times exopod of uropod. Spines on lateral margins continuously increase in size from half-length to 3/4-length of lateral margins and then decrease weakly in size distally. Laminae of the cleft are shorter than the pair of disto-mesial spines flanking the cleft. For additional details, see "Diagnosis."

Nauplioid larvae (Fig. 9C, D) with three pairs of free naupliar appendages. Apical portions of antennulae, antennae, and abdomen with minute hairs.

Discussion

The new species clearly belongs to the genus *Ischiomysis* by modified setae of the carpopropodus and apically bifid claw of thoracic endopod 4 in both sexes, as well as by modified praeischium and subapically flagellate spines on the ischium of endopod 8 in males. It differs from both so far known congeners by apically incised rostrum in both sexes, by two versus only one flagellate spine on the ischium of endopod 8 in males, and by additional characters outlined in Table 1.

Due to the short distance (only 37 km air route and >40 km waterways) between the type locality of *I. telmatactiphila* at the coast of the Island of São Tomé and that of *I. proincisa* sp. nov. off the only 2-km distant, much smaller Ilhéu das Rolas, these two species are considered sympatric. The third species of this genus, *I. peterwirtzi* from the Cape Verde Islands, is geographically and also morphologically "remote" from both its congeners by the handle of the flagellate spines on the antennular peduncle and on the carpus of thoracic endopod 3 not ending in a spiniform projection, by carpus 3 bearing fewer flagellate spines, by lateral margins of the telson on average with longer bare portion, and telson cleft shorter and with longer portion lined by laminae. The allopatric *I. telmatactiphila* and *I. peterwirtzi* share an association (less close in *I. peterwirtzi*) with the club-tipped anemone *Telmatactis cricoides*, whereas the two sympatric species are ecologically more remote due to the anemone association of *I. telmatactiphila* in well-lit habitats versus *I. proincisa* sp. nov. dwelling in a comparatively large semi-dark cave without anemones.

An incised anterior margin of the carapace is rare but not exceptional within the Mysidae. It is also known from *Neomysis ilyapai* Holmquist, 1957, belonging to the subfamily Mysinae, phylogenetically remote from the present new species, which belongs to the Heteromysinae. The former species is endemic to the coasts of Chile. A slightly depressed mid-anterior margin of the carapace is found in *N. rayii* (Murdoch, 1885) from the N-Pacific and Arctic seas and in *N. czerniavskii* Derzhavin, 1913, from the NW- and N-Pacific.

Acknowledgements

The Centro de Ciencias do Mar, University of the Algarve, co-financed several trips of the second author to São Tomé and to the Cape Verde Islands. This study received Portuguese national funds through FCT—Foundation for Science and Technology—through projects UIDB/04326/2020, UIDP/04326/2020, and LA/P/0101/2020.

References

Alcaraz M, Riera T, Gili JM (1986) *Hemimysis margalefi* sp. nov. (Mysidacea) from a submarine cave of Mallorca Island, western Mediterranean. Crustaceana 50(2): 199–203. https://doi.org/10.1163/156854086X00214

Bhaduri RN, Crowther AL (2016) Association of the mysid *Idiomysis inermis* with the sea anemone *Stichodactyla haddoni* in Moreton Bay. Marine Biodiversity 46: 707–711. https://doi.org/10.1007/s12526-015-0408-7

Daneliya ME (2021) On the mysid crustacean genus *Heteromysis* (Mysidae: Heteromysinae) of the Tasman Sea, with notes on the Tribe Heteromysini. Records of the Australian Museum 73: 1–50. https://doi.org/10.3853/j.2201-4349.73.2021.1737

Derzhavin AN (1913) Neue Mysiden von der Küste der Halbinsel Kamtschatka. Zoologischer Anzeiger 43: 197–204. https://www.zobodat.at/pdf/ZoologischerAnzeiger_43_0197-0204.pdf

Duchassaing de Fonbressin P (1850) Animaux Radiaires des Antilles. Plon Frères, Paris, 35 pp.

Holmquist C (1957) Mysidacea of Chile. Reports of the Lund University Chile Expedition 1948–1949. Lunds Univeristets Årsskrift, N.F. Adv. 2, 53(6): 1–53.

Ledoyer M (1963) *Hemimysis speluncola* n.sp. Mysidacé nouvelle des grottes sous-marines obscures. Recueil des Travaux de la Station Marine d'Endoume 30: 77–81.

Mauchline J (1980) The biology of mysids and euphausiids. In: Blaxter JHS, Russell FS, Young M (Eds) Advances in Marine Biology, Academic Press, London, Vol. 18, 1–677.

Mees J, Meland K [Eds] (2024) World List of Lophogastrida, Stygiomysida and Mysida. In: World Register of Marine Species. Instant Web Publishing. https://www.marinespecies.org/aphia.php?p=taxdetails&id=1379689

Murdoch J (1885) Description of seven new species of Crustacea and one worm from Arctic Alaska. Proceedings of the United States National Museum 7: 518–522. https://doi.org/10.5479/si.00963801.459.518

Norman AM (1892) On British Mysidae, a family of Crustacea Schizopoda. Annals and Magazine of Natural History, ser. 6, 10(56): 143–166. https://doi.org/10.1080/00222939208677385

Nouvel H (1942) Diagnoses préliminaires de Mysidacés nouveaux provenant des campagnes du Prince Albert 1er de Monaco. Bulletin de l'Institut Océanographique de Monaco 831: 1–12. www.vliz.be/imisdocs/publications/261362.pdf

Riera T, Zabala M, Peñuelas J (1991) Mysids from a submarine cave emerge each night to feed. Scientia Marina 55: 605–609. https://diposit.ub.edu/dspace/bitstream/2445/32435/1/121050.pdf

Saito N, Hoshino O, Fukuoka K (2018) First record of *Pleurerythrops secundus* (Crustacea, Mysida) in association with benthic hydroids (Cnidaria, Hydrozoa) in shallow water of Izu-Ohshima, Pacific coast of central Japan. Crustacean Research 47: 137–143. https://doi.org/10.18353/crustacea.47.0_137

San Vicente C, Monniot F (2014) The ascidian-associated mysid *Corellamysis eltanina* gen.nov., sp.nov. (Mysida, Mysidae, Heteromysinae): a new symbiotic relationship from the Southern Ocean. Zootaxa 3780(2): 323–346. https://doi.org/10.11646/zootaxa.3780.2.6

Wilson GDF (1989) A systematic revision of the deep-sea subfamily Lipomerinae of the isopod crustacean family Munnopsidae. Bulletin of the Scripps Institution of Oceanography 27: 1–138.

Wittmann KJ (1978) Biotop- und Standortbindung mediterraner Mysidacea. Doctoral thesis, Univ. Vienna, 1–211.

Wittmann KJ (1981) Comparative biology and morphology of marsupial development in *Leptomysis* and other Mediterranean Mysidacea (Crustacea). Journal of experimental marine Biology and Ecology 52: 243–270. https://doi.org/10.1016/0022-0981(81)90040-X

Wittmann KJ (2013) Mysids associated with sea anemones from the tropical Atlantic: descriptions of *Ischiomysis* new genus, and two new species in this taxon (Mysida: Mysidae: Heteromysinae). Crustaceana 86: 487–506. https://doi.org/10.1163/15685403-00003166

Wittmann KJ (2020) Lophogastrida and Mysida (Crustacea) of the "DIVA-1" deep-sea expedition to the Angola Basin (SE-Atlantic). European Journal of Taxonomy 628: 1–43. https://doi.org/10.5852/ejt.2020.628

Wittmann KJ (2023) Evidence and modification of non-visual eyestalk organs in troglobiont Mysida and Stygiomysida (Crustacea). Arthropoda 1(4): 432–450[, suppl.]. https://doi.org/10.3390/arthropoda1040019

Wittmann KJ (2024) Mysidae (Crustacea: Mysida) from sponges in sublittoral waters of Lizard Island (Indo-Pacific: Coral Sea), with description of *Heteromysis kaufersteinae* sp. nov., first record of *H. domusmaris* from nature, and range extension in *Anchialina lobata*. Crustacean Research 53: 97–111. https://doi.org/10.18353/crustacea.53.0_97

Wittmann KJ, Ariani AP (2019) Amazonia versus Pontocaspis: a key to understanding the mineral composition of mysid statoliths (Crustacea: Mysida). Biogeographia – The Journal of Integrative Biogeography 34: 1–15. https://doi.org/10.21426/B634142438

Wittmann KJ, Chevaldonné P (2021) First report of the order Mysida (Crustacea) in Antarctic marine ice caves, with description of a new species of *Pseudomma* and investigations on the taxonomy, morphology and life habits of *Mysidetes* species. ZooKeys 1079: 145–227. https://doi.org/10.3897/zookeys.1079.76412

Wittmann KJ, Griffiths CL (2017) Three new species of *Heteromysis* (Mysida, Mysidae, Heteromysini) from the Cape Peninsula, South Africa, with first documentation of a mysid-cephalopod association. ZooKeys 685: 15–47. https://doi.org/10.3897/zookeys.685.13890

Wittmann KJ, Wirtz P (2017) *Heteromysis sabelliphila* sp. nov. (Mysida: Mysidae: Heteromysinae) in facultative association with sabellids from the Cape Verde Islands (subtropical N.E. Atlantic). Crustaceana 90: 131–151. https://doi.org/10.1163/15685403-00003624

Wittmann KJ, Ariani AP, Lagardère J-P (2014) Chapter 54. Orders Lophogastrida Boas, 1883, Stygiomysida Tchindonova, 1981, and Mysida Boas, 1883 (also known collectively as Mysidacea). In: von Vaupel Klein JC, Charmantier-Daures M, Schram FR (Eds) Treatise on Zoology - Anatomy, Taxonomy, Biology. The Crustacea. Revised and updated, as well as extended from the Traité de Zoologie, Koninklijke Brill NV, Leiden, Vol. 4 Part B: 189–396. https://doi.org/10.1163/9789004264939_006

Wittmann KJ, Abed-Navandi D, Dubois M, Chevaldonné P (2021) Three new species of *Heteromysis* (Crustacea: Mysida) from coral reef aquaria in Florida and Central Europe. Zootaxa 4980: 490–520. https://doi.org/10.11646/zootaxa.4980.3.3